Copper^{2+} Binding to α-Synuclein. Histidine50 can form a ternary complex with Cu^{2+} at the N-terminus but not a macrochelate.

Yao Tian‡^, Helen F. Stanyon‡^, Joseph D Barritt‡^$, Uroosa Mayet^, Pelak Patel^, Elena Karamani^, Giuliana Fusco£ and John H. Viles^†

^School of Biological and Chemical Sciences, Queen Mary, University of London

Mile End Road, London E1 4NS, United Kingdom

$ Department of Life Sciences, Imperial College London, London SW7 2AZ, United Kingdom

£ Centre for Misfolding Diseases, Department of Chemistry, University of Cambridge, Cambridge, CB1 1EW, United Kingdom

‡ Authors have contributed equally to this manuscript

†Corresponding Author

KEYWORDS Parkinson's Disease; Synuclein; Copper; Cu^{2+}; Circular Dichroism; coordination; affinity; macrochelate; ternary complex; N-terminus; pH; amyloid; fibril; dissociation constant; peptide; CD

Supporting Information

ABSTRACT: Alpha-synuclein (αSyn) forms amyloid fibrils in the neurons of Parkinson's disease (PD) patients'. Despite a role for Cu^{2+} in accelerating αSyn fibril formation, coupled with reports of copper dis-homeostasis in Parkinson's disease (PD), there remain controversies surrounding the coordination geometry of Cu^{2+} with αSyn. Here we compare visible circular dichroism (CD) spectra of Cu^{2+} loaded on to full-length αSyn together with four peptides that model aspects of Cu^{2+} binding to the N-terminus and Histidine50 of αSyn. Using glycine as a competitive ligand, the affinity of Cu^{2+} for full-length αSyn is determined to have a conditional dissociation constant, at pH 7.4, of 0.1 nM. A similar affinity of 0.3 nM is determined for the tri-peptide MDV that mimics the N-terminus of αSyn, while the incorporation of a putative histidine side-chain in the N-terminal complex facilitates the formation of a macro-chelate with the histidine, which results in an increase in the affinity for Cu^{2+} to 0.03 nM at pH 7.4. Comparisons of the visible absorbance and CD spectra over a range of pH values also indicates that the MDV tripeptide closely models Cu^{2+} binding to full-length αSyn and rules out a role for His50 in the primary Cu^{2+} binding complex of monomeric αSyn. However, there are reports that suggest His50 does form a macro-chelate with the N-terminal Cu^{2+} complex; we reconcile these conflicting observations by identifying a concentration dependence of the interaction. Only at the higher concentrations can the imidazole nitrogen bind to the N-terminal Cu^{2+} to from a ternary complex, rather than via a macrochelate. This work shows even for this intrinsically disordered protein a large macro-chelate with Cu^{2+} is not favored. Understanding Cu^{2+} coordination to αSyn gives a more complete picture of its place in amyloid assembly and cytotoxicity

INTRODUCTION:

Parkinson's disease (PD) is the second most prevalent neurodegenerative disorder after Alzheimer's disease. PD is marked by the loss of dopaminergic neurons in the brain's *substantia nigra,* along with the presence of subcellular protein accumulations, known as Lewy bodies. These Lewy bodies are comprised of amyloid fibrils of the protein alpha-synuclein (αSyn). Furthermore, some early onset inherited forms of PD are associated with single point mutations within αSyn, for example: A53T; A30P; E46K; H50Q [1]. Metal ions, and in particular copper ions, have been linked with PD through the observation of increased Cu^{2+} concentrations in the cerebrospinal fluid of PD patients [2], while those with chronic exposure to copper in industry have an increased risk of developing PD [3].

αSyn is largely found intracellularly at presynaptic terminals in the reducing environment of the cytosol where copper ions are predominantly Cu^{+}. There have been a number of studies of Cu^{+} coordination to αSyn [4a , 4b , 4c]. In addition, Cu ions are capable of redox cycling between Cu^{+} and Cu^{2+} which can lead to hydroxyl radical production and other reactive oxygen species, a hallmark of PD [5]. Indeed, hydroxyl radical production by copper redox cycling can cause dityrosine formation in αSyn, which can affect amyloid assembly [6]. A proportion of αSyn is secreted by neuronal cells extracellularly [7] which highlights the importance of Cu^{2+} binding to αSyn.

The coordination of Cu^{2+} can affect the structure and self-assembly of αSyn. The change in charge may affect the self-association, while Cu^{2+} coordination can affect the amyloid assembly pathway [8] and structural morphologies (strain) of the amyloids fibrils [9] . Cu^{2+} has been proposed as a trigger for the misfolding and assembly of αSyn in Parkinson's disease (PD) as Cu^{2+} can accelerate αSyn fibril formation *in vitro* [8, 9c, 10]. Cu^{2+} has also been shown to exacerbate toxicity

of oligomeric αSyn in cell cultures [9b, 9c] . It is for these reasons much effort has been directed at characterizing the coordination and affinity of Cu^{2+} binding to αSyn, for reviews see [4b, 4c, 11] .

Visible CD is a powerful probe of coordination in metal ion-protein complexes. The coordination of Cu^{2+} via amide main-chain chelation generates CD signal in the d-d electronic absorption bands, known as the vicinal effect. The sign of the signal is very sensitive to the coordination geometry [12]. One advantage Vis-CD has over visible absorption spectra is that the non-protein bound metal ion is typically CD silent. As a consequence, determination of the stoichiometry, coordination geometry and pH dependence of metal ion binding is not complicated by signal from the free metal ion [10a, 13].

αSyn is 140 residues in length and is intrinsically disordered in an aqueous environment. Paramagnetic broadening by Cu^{2+} of ^{1}H-^{15}N HSQC NMR spectra of full-length αSyn identified 3 regions of the protein that interact with Cu^{2+} ions. These were centered at the N-terminus; His50 and Asp121 [10a, 14] , although paramagnetic broadening by Cu^{2+} can be caused by weak transient Cu^{2+} binding. Numerus studies have now shown the locus of the primary binding site for Cu^{2+} to be the N-terminal amino group [4b] . These include spectroscopic [15 16] and potentiometric studies [15b 16d] of peptide models and comparisons with full-length αSyn. It has been suggested that αSyn binds Cu^{2+} ions through two different modes; solely at the N-terminal residues MDV, see Figure 1a [15] or alternatively, via the N-terminal residues together with the imidazole of histidine at position 50 to form a macro-chelate complex, Figure 1b [16]. While model peptides of the N-terminus (MDV), together with free imidazole, have been shown to form a ternary Cu^{2+} complex at high pH [17]. Post-translational modifications of αSyn where the N-terminus becomes acetylated have been reported [18 19]. Although quantitation is difficult, the acetylation of the N-terminus is

believed to be quite wide spread, but is not thought to be universal. The primary binding site for Cu^{2+} for acetylated αSyn is centered at His50 not at the N-terminal residues [20].

We aim to build on the large body of work surrounding the coordination of Cu^{2+} to αSyn, and resolve some of the controversies surrounding the role of His50 in the primary N-terminal binding site. To investigate the influence of the side chains, Asp2 and His50, on Cu^{2+} binding to the N-terminus of αSyn, four peptides models were generated: (i) αSyn(1-3) (MDV-am); (ii) αSyn(1-3D2A) (MAV-am); (iii) αSyn(ac46-52) (ac-EGVVHGV-am); and (iv) αSyn(1-7,46-52) (MDVFMKGEGVVHGV-am). The affinities, visible-CD, absorption spectrum and pH dependence of coordination and are directly compared with Cu^{2+} binding to full-length αSyn. We show the affinity, pH dependence, absorbance and visible-CD spectra for full-length, αSyn is most similar to that of the tri-peptide MDV, and the histidine side-chain at position 50 does not coordinate to the primary Cu^{2+} binding site in full-length αSyn by forming a macro-chelate.

EXPERIMENTAL

Expression and Purification of αSyn:

αSyn was expressed and purified as previously described [21]. Briefly the protein was expressed in *E. coli* using plasmid pT7-7 [21] . After transforming in BL21 (DE3)-gold cells (Agilent Technologies, Santa Clara, USA), αSyn was obtained by growing the bacteria in LB at 37 °C under constant shaking at 250 rpm and supplemented with 100 $\mu g \cdot ml^{-1}$ ampicillin to an OD of 0.6. The expression was induced with 1 mM isopropyl β-D-1-thiogalactopyranoside (IPTG) at 37 °C for 4 h, and the cells were harvested by centrifugation at 6200 *g* (Beckman Coulter, Brea, USA). The cell pellets were re-suspended in lysis buffer (10mM Tris-HCl pH 8, 1 mM EDTA and EDTA-free complete protease inhibitor cocktail tablets obtained from Roche, Basel, Switzerland) and lysed by sonication. The cell lysate was centrifuged at 22,000 *g* for 30 min to remove cell debris. In order to precipitate the heat-sensitive proteins, the supernatant was then heated for 20 min at 70 °C and centrifuged at 22,000 *g*. Subsequently streptomycin sulfate was added to the supernatant to a final concentration of 10 $mg \cdot ml^{-1}$ to stimulate DNA precipitation. The mixture was stirred for 15 min at 4°C followed by centrifugation at 22,000 *g*. Then, ammonium sulfate was added to the supernatant to a concentration of 360 $mg \cdot ml^{-1}$ in order to precipitate the protein. The solution was stirred for 30 min at 4°C and centrifuged again at 22,000 *g*. The resulting pellet was re-suspended in 25 mM Tris-HCl, pH 7.7 and dialyzed against the same buffer in order to remove salts. The dialyzed solutions were then loaded onto an anion exchange column (26/10 Q sepharose high performance, GE Healthcare, Little Chalfont, UK) and eluted with a 0–1 M NaCl step gradient, and then further purified by loading onto a size exclusion column (Hiload 26/60 Superdex 75 preparation grade, GE Healthcare, Little Chalfont,

UK). All the fractions containing the monomeric protein were pooled together and concentrated by using Vivaspin filter devices (Sartorius Stedim Biotech, Gottingen, Germany). The purity of the aliquots after each step was analyzed by SDS-PAGE and the protein concentration was determined from the absorbance at 275 nm using an extinction coefficient of 5600 M^{-1} cm^{-1}.

Peptides and Proteins:

Peptides were purchased from Generon Ltd (Maidenhead, UK). F-moc chemistry was used to synthesize the various model peptides. All peptides were C-terminally amidated in order to mimic the continuation of the peptide sequence in the larger protein. The peptides were removed from the resin and de-protected before purification to a single elution band by reverse-phase HPLC. The samples were characterized using mass spectrometry.

Peptides with amidated C-termini (am) and free N-terminal amino groups studied included MDV, MAV, ac-EGVVHGV (with acetylated N-terminus; αSyn(ac46-52)) and MDVFMKGEGVVHGV; a designed sequence based on α-synuclein residues 1-7 and 46-52; αSyn(1-7,46-52).

UV-Visible Absorption spectroscopy:

UV-Visible electronic absorption spectra of the Cu^{2+} complexes were acquired using a Hitachi U-3010 spectrophotometer using a 1 cm path-length (l) quartz cuvette. Spectra were acquired between 200-800 nm with a wavelength scan speed of 60 nm $mins^{-1}$. Absorption spectra were smoothed using a 6 nm window and adjusted for concentration (c); $\varepsilon = Abs/(c \cdot l)$.

Circular Dichroism (CD):

Typically, CD spectra were recorded at 25° C on an Applied Photophysics Chirascan instrument between 260 and 800 nm, with sampling points every 2 nm, using a 1 cm pathlength cell. Typically, three scans were recorded and averaged, baseline spectra subtracted from each spectrum, followed by smoothing using a window of 6 nm. Data were processed using Applied Photophysics Chirascan Viewer, Microsoft Excel and the KaleidaGraph spreadsheet / graph package. The molar ellipticity $\Delta\varepsilon$ ($M^{-1}cm^{-1}$), spectra were obtained through conversion of the direct CD measurements (θ, in millidegrees), using the relationship $\Delta\varepsilon = \theta/(c * l * 33{,}000)$, where c is the molar concentration and l is the path-length.

Titrations:

All chemicals were purchased from Sigma-Aldrich at the highest purity available and UHQ water was used throughout (10^{-18} $\Omega^{-1}cm^{-1}$ resistivity). Small aliquots of fresh 20 mM aqueous solutions (Cu^{2+} as $CuCl_2.2H_2O$,) and glycine were used for titrations. Typically ethylmorpholine buffer (20 mM) was used in measurements presented in figures 2, 3, 4 and S1. While pH dependence spectra, Figure 5 and also Figure 6, S2-S7 were recorded in the absence of a buffer. The pH was adjusted with µl additions of 0.05 mM NaOH or HCl. pH was maintained to within 0.05 of a pH unit. The pH was measured before and after acquiring each spectrum. The lyophilized weight of each peptide was used to estimate the concentration, assuming 20 % moisture content. However, it was the known concentration of metal ions at sub-stoichiometric levels to the peptide that was used for the conversion to molar ellipticity.

Affinity measurements:

Glycine, the competing Cu^{2+} chelator used in calculating the affinity of the Cu^{2+}-peptide complexes, forms a $Cu(Gly)_2$ complex when bound to Cu^{2+}. The individual conditional affinities of each glycine binding event (K_{a1} and K_{a2}), at pH 7.4, are $7.4x10^5$ and $7.4x10^4$ M^{-1} respectively[22].

The concentration of Gly required for equal mole equivalents of Cu^{2+} to be bound to both peptide and glycine is used to determine the affinity (conditional dissociation constants) at pH 7.4 of Cu^{2+} for the protein using equation 1. The "free" Cu^{2+} refers to the concentration of Cu^{2+} not bound to either glycine or peptide.

$$K_d = [Cu^{2+}_{free}] = \frac{[Cu^{2+}_{total}] - [Cu^{2+}_{bound\ to\ peptide}]}{1 + (K_{a1}[Gly_{free}]) + \left(K_{a1}K_{a2}\left([Gly_{free}]^2\right)\right)}$$

(Equation 1)

Where; Cu^{2+} bound to peptide is equal to total Cu^{2+} (at $\theta = 0.5$) divided by 2 and $[Gly_{free}] = [Gly_{total}] - [Gly_{bound\ to\ Cu^{2+}}]$.

RESULTS:

Cu^{2+} affinity of αSyn and peptide models

The Cu^{2+} affinity of the four peptides which model aspects of Cu^{2+} coordination to αSyn have been studied. The affinities have been determined at pH 7.4 using glycine as a competitive ligand and directly compared to full-length αSyn (Figure 2, Table 1). The amount of glycine needed to compete Cu^{2+} from the αSyn peptides can be used to calculate the affinity by monitoring the Visible-CD signal of Cu^{2+} bound to the αSyn peptides. This approach has the advantage of directly monitoring the coordination of Cu^{2+} to the model peptides, while the $Cu(Gly)_2$ complex is CD-silent, and has a known affinity for Cu^{2+}. We note, there is no shift in wavelength of the absorption bands upon addition of glycine which indicates a ternary complex is not favored, and so glycine is a direct competitor for Cu^{2+}. The difference in affinity for the four peptide models is quite marked. In particular, 8.5 molar equivalents of glycine, is required to remove half of the Cu^{2+} from MDV tri-peptide (Figure 2a) while only 1.2 molar equivalents of glycine are required to remove half of the Cu^{2+} from MAV (Figure 2b). Using equation 1 (see experimental) a conditional dissociation constant (K_d) at pH 7.4 can be calculated. Cu^{2+} affinities for the various peptide models are summarized in Table 1. The conditional dissociation constants, at pH 7.4, range between 30 pM and 18 μM. Notably, the Cu^{2+} complex at the N-terminus involving Asp2 and chelation from histidine imidazole is an order of magnitude tighter, at 0.03 nM compared to the N-terminal tripeptide complex MDV, 0.3 nM. In contrast, the peptide which contains just His50 as a residue with a Cu^{2+} coordinating sidechain, has an affinity for Cu^{2+} six orders of magnitude weaker with a K_d of 18 μM.

The Cu^{2+} affinities for the 4 peptide models can be directly compared to full-length αSyn, Figure 2e. The affinity for full-length αSyn is slightly tighter than that of the tri-peptide MDV,

0.3 nM, compared to 0.1 nM for full-length αSyn, while the peptide containing a histidine to form a macro-chelate has an affinity 3 times tighter (0.03 nM) than full-length αSyn. To summarize, the Cu^{2+} affinity for full-length αSyn is closest in magnitude to two model peptides; MDV and the macro-chelate complex MDV with the additional histidine residue, Table 1.

Table 1. Comparison of Cu^{2+} binding affinities and wavelength absorption properties for αSyn and model peptides

Protein/peptide	**K_d at pH 7.4**	**λ max absorption**	**λ max CD**
αSyn(1-140)	0.1 nM	628 nm (pH 5.5 - 9)	610 nm (+)
MDV	0.28 nM	628 nm (pH 5.5 - 9)	618 nm (+)
αSyn(1-7,46-52)	0.03 nM	605 nm (pH 7.5 - 9) 628 nm (pH 5.5)	570 nm (+) (pH 7.5 - 9) 610 nm (pH 5.5)
MAV	36 nM		555 nm (-)
αSyn(ac46-52)	18000 nM	590 nm	525 nm (+)

K_d are conditional dissociation constant, at pH 7.4, spectra reported at pH 7.4 unless stated.

Visible Absorbance and CD Spectra

Next we compared the visible absorbance spectra and visible-CD spectra of the model peptides to full-length αSyn. The difference in Cu^{2+} coordination geometries is reflected in the visible absorbance spectra shown for Cu^{2+} loaded at 0.9 mol equivalents, at pH 7.4, Figure 3a. In particular, an increase in the number of coordinating nitrogens in the Cu^{2+} tetragonal complex

will result in absorbance maxima at shorter wavelengths, for the d-d electronic transitions. For example, absorbance bands range between 540 nm for the 4N complexes to 765 nm for a 1N3O complex [23]. This behavior is observed for the αSyn model peptides; the MDV Cu^{2+} complex has been shown to form a 2N2O complex (Figure 1a) and has an absorption band centered at 630 nm, as would be predicted, while the macro-chelate complex αSyn(1-7,46-52), which forms a 3N1O coordination (Figure 1b) is shifted to shorter wavelengths and has an absorption maximum at 605 nm, see Fig 3a. The absorption spectrum of full-length αSyn is almost identical to that of the absorbance spectrum for MDV, Figure 3a.

Visible-CD spectra are very sensitive to coordination geometry around Cu^{2+} and so can give additional information beyond the visible absorbance spectra, whilst not being complicated by signal from the presence of unbound Cu^{2+} [10a, 13]. The visible-CD spectra of all four peptides are shown in Figure 3b,c, loaded with 0.9 mol-equivalents of Cu^{2+} at pH 7.4, and compared with full-length αSyn. The MDV analogue, with an Asp2Ala substitution, has marked effects on the CD spectra, causing an inversion of the vis-CD spectra for the d-d electronic transition, as previously reported [15a]. Although not identical, the spectrum of αSyn has the closest similarity with MDV, with CD bands centered at 610 and 625 nm respectively, Fig 3c. The visible-CD spectrum of αSyn(1-7,46-52) which can form the macro-chelate with the histidine side-chain also has similarities to full-length but like the absorption spectrum the CD band is shifted to a shorter wavelength, with a visible-CD maxima at 570 nm. The CD signal of the αSyn(ac46-52) model peptide is very different with a positive CD band at 540 nm. The CD absorbance bands observed are also summarized in Table 1.

Stoichiometry of Cu^{2+} Coordination

To further probe the Cu^{2+} coordination to the model peptides, Cu^{2+} has been loaded on to the peptides beyond 1 mole equivalent. Titration of Cu^{2+} on to MDV and MAV at pH 7.4 shows a clear 1:1 stoichiometry with fixed CD bands, centered at 612 and 555 nm, respectively, that increase in intensity until saturation at 1 mole equivalent, shown in Supplemental Figure S1a,b. Similarly, the αSyn(ac46-52) peptide also forms a 1:1 complex with a single set of CD signal at 520 nm and 320 nm (Supplemental Figure S1c). In contrast, the Cu^{2+} binding properties of αSyn(1-7,46-52) are more complicated with a CD band at 573 nm that increases in intensity up to one molar equivalent of Cu^{2+}, this CD band then reduces a little in intensity while a CD band centered at 543 nm appears, Figure 4a. Addition of a second Cu^{2+} ion shifts the CD band towards a shorter wavelength of 543 nm, this change in wavelength maxima in the CD spectra between 1 and 2 mole equivalents of Cu^{2+} is shown as an insert in Fig 4a. We postulated that the macro-chelate complex composed of the N-terminus and histidine is replaced by two separate complexes at two equivalents of Cu^{2+}, with the two separate complexes centered at MDV and His50, as previously suggested [17]. This possible behavior is strongly supported by simulated data presented in Figure 4b, here the spectrum of αSyn(1-7, 46-52) with two equivalents of Cu^{2+} can be very closely mimicked by the direct combination of two individual CD spectra of MDV and αSyn(ac46-52) at 1 equivalent, as shown in Figure 4b. This Cu^{2+} titration indicates the coordination geometry is sensitive to changes in Cu^{2+} stoichiometry with loss of the macro-chelate at supra-stoichiometric equivalents.

pH dependence of Cu^{2+} binding: histidine coordination is lost at low pH.

The pH dependence of Cu^{2+} binding to the MDV tripeptide and αSyn(1-7,46-52) are shown in Figure 5. These are highlighted because they have the most similar CD, absorbance spectra and affinity to full-length αSyn, which is also shown in Figure 5. Figure 5a-c shows visible absorption spectra while Fig 5d-f shows the complementary visible-CD spectra over a range of pHs in the presence of 1 mol-equivalent of Cu^{2+}. A single set of visible-CD bands for MDV remain very stable over a range of pHs (between pH 5-10), there is no indication of a shift to other coordination geometries with an increase in pH. The mid-point of Cu^{2+} complex formation occurs at a relatively low pH of 4.6 for MDV (Figure 5a). It is clear that the Asp has a significant stabilising influence on the complex even at relatively low pH values, as previously described [15a].

The behavior of αSyn(1-7, 46-52) coordination is more complex. At pH 7 and above the visible absorption spectra are consistent with a 3N1O geometry which has an absorbance maximum at 600 nm. Below pH 7 the absorbance maxima shifts to longer wavelengths from 600 to 630 nm, Figure 5b, which is consistent with 2N2O coordination. This shift to longer wavelengths at lower pH values is echoed in the Visible-CD spectra which shifts from 605 to 630 nm for the CD bands, Figure 5e. The αSyn(1-7, 46-52) visible-CD bands below pH 6 adopt the same appearance as the MDV tripeptide. This suggests a change in coordination from 3N1O complex (pH 7.0) to a 2N2O complex at lower pH (pH 5.5). This behavior indicates the loss of the macro-chelate imidazole ligand between pH 5.5-7. The pH dependence spectra of full-length αSyn resembles much more closely the behavior of MDV than the αSyn(1-7,46-52) peptide. In particular, there is no marked-shift in absorbance maximum between pH 7 and 5.5. Like the MDV tripeptide the absorbance bands remains centered at 630 nm over the whole range of pHs

for full-length αSyn. This is strong evidence to rule out any significant role for coordination by His50 in full-length αSyn Cu^{2+} complex even at high pH.

The pH dependent Vis-CD spectra of Cu^{2+} complexes for MAV is shown as supplemental data, Figure S2, and is very different from the behavior of full-length αSyn. In the case of MAV, which lacks aspartate, the Vis-CD spectra suggests a complete loss of amide Cu^{2+} coordination below pH 7, with a mid-point at pH 7.5. This type of pH dependence for MAV is similar to the tripeptide AAA [12b]. The αSyn(ac46-52) Cu^{2+} complex is also very pH sensitive with the loss of a CD active complex below pH 6 implying a loss of amide main-chain coordination, Supplemental Figure S2b.

Concentration dependence of imidazole chelation to the N-terminal Cu^{2+} complex

Our absorption and visible CD data indicates the His50 does not bind to the N-terminal Cu^{2+} complex in full-length αSyn, and yet there are two quite careful studies using multi-pulse EPR to indicate His50 does coordinate in full-length αSyn [16a 16b]. We wondered how these conflicting observations could be reconciled. We postulated the differences observed might be related to the differences in experimental conditions. In particular, the EPR spectra were acquired at much higher concentrations in the presence of the cryo-protectant glycerol. We questioned if the glycerol might impact the αSyn structure and its ability to form a macro-chelate. We therefore obtained visible-CD and absorbance spectra of Cu^{2+} loaded αSyn in the presence of 25% (v/v) glycerol. Comparison of the absorption spectra and visible-CD indicate glycerol does not affect the coordination of the Cu^{2+}, see Supplemental Figure S3, which rules this out as an explanation of the conflicting binding modes reported.

Next, we determined whether higher concentrations (350 μM) used in the EPR experiments could explain the different behavior. Full-length αSyn is poorly soluble so it was not possible to study using optical spectroscopy, however it was possible to use the more soluble MDV model peptide over a range of concentrations between 500 μM (used in the EPR experiments) to 100 μM used here in the visible absorption/CD experiments. We studied the ternary complex of MDV: Cu^{2+}: αSyn(ac46-52) (1:1:1) over a range of concentrations A clear concentration dependence of the wavelength maxima in both the visible-absorption and visible-CD spectra is observed, Figure 6. We also show a very similar concentration dependent behavior for the mixture of MDV: Imidazole: Cu^{2+} (1:1:1), shown as supplemental Figure S4. The impact of imidazole on the Cu-MDV visible absorption spectra are also shown in supplemental Figure S5. This ternary 3N1O complex with imidazole has previously been described [17]. Our spectra indicate, the more concentrated the (1:1:1) mixture, the more the absorbance bands shifted to shorter wavelengths. The shift to shorter wavelengths at higher concentrations suggests an increase in the extent of nitrogen (imidazole) equatorial chelation as the water oxygen is displaced. The concentration dependent behavior of the ternary complex, Figure 6 and S4, gives an explanation for the differing reports of His50 involvement in the N-terminal complex of full-length αSyn.

To confirm a role for the imidazole chelation of Cu^{2+} at higher concentrations control experiments were performed with MDV and Cu^{2+} only. As expected the spectra shows no concentration dependent behavior, supplemental Figure S6. We also performed concentration dependent measurements for αSyn(1-7,46-52), supplemental Figure S7. This peptide exhibits absorbance bands typical for a 3N1O complex over all concentrations. This concentration

independent behavior supports the assertion that αSyn(1-7,46-52), with just 12 amino acids between the histidine and the N-terminus, forms a macro-chelate rather than a ternary complex.

DISCUSSION:

To resolve controversies surrounding Cu^{2+} coordination to αSyn we have compared affinity, visible absorbance, visible CD, and pH dependence behavior for full-length αSyn to that of a series of model peptides. Taking this data together, the peptide model that most closely mimics Cu^{2+} binding to full-length αSyn is that of the simple tripeptide MDV, Figure 7a. The lack of pH dependence changes of full-length αSyn for visible absorbance and visible CD spectra rules out the formation of the complex with His50. In contrast, αSyn(1-7,46-52) does have imidazole nitrogen coordination at pH 7.4 which begins to be lost at pHs below 7 and is completely lost by pH 5.5, Figure 7b. The different behavior of αSyn(1-7,46-52) model peptide compared to full-length αSyn can be explained by the considerable reduction in the number of residues between the N-terminus and the Histidine to just 12 residues in the model peptide. This facilitates histidine sidechain coordination in the N-terminal complex. We show here that higher pHs and sub-stoichiometric ratios of Cu^{2+} will promote the macro-chelate in the model peptide αSyn(1-7,46-52), however even under these conditions our data indicates the His50 macro-chelate does not form for full-length αSyn. The visible absorption spectra are essentially identical for Cu^{2+} bound to MDV and full-length αSyn over the entire pH range 5-9. There are however subtle differences in the Cu^{2+} Vis-CD spectra, these may reflect very small differences in the conformation of the main-chain in the plain of the copper complex [12], caused by the presence of the additional 140 residues, rather than differences in the coordinating ligands. The involvement

of His50 (at 100 μM αSyn) can be ruled out as there are no pH dependent changes in coordination between pH 5.5 and 7.

So why have some studies reported His50 involvement in the primary N-terminal Cu^{2+} complex? There are two key studies using EPR and full-length αSyn that suggest this involvement [16a, 16b]. Drew *et al* points to a mixture of both 3N1O and 2N2O coordination geometries (Figure 1a and 1b) in approximately equal proportions at pH 7.4 [16a]. Their relative proportions are likely to be pH sensitive, indeed, an EPR study at pH 6.5 indicates a single set of EPR signals for the 2N2O complex [15a]. An explanation for the different observations compared to the data presented here, simply arises from the experimental condition, when acquiring EPR spectra. In particular the EPR spectra are acquired at 350 μM of αSyn, these high concentrations favor displacement of the water with His50 imidazole from a second αSyn molecule, Figure 7c. This assertion is supported by the concentration dependent behavior of the model ternary system, (MDV + αSyn(ac46-52) + Cu^{2+}), shown in Figure 6. Only at the higher concentrations can the imidazole displace the water. This concentration dependent behavior can explain the change in coordination from 2N2O at low concentration to 3N1O at higher concentration. This also suggests that rather than full-length αSyn forming a macrochelate, whose formation would be independent of concentration, the His50 coordination is derived from a second αSyn molecule only favored at higher concentrations.

We note that in full-length αSyn, His50 is covalently linked to the N-terminus, this will increase the 'effective concentration' of His50 close to the N-terminus in this intrinsically disordered protein. However, this is not sufficient to overcome the significant ordering necessary to form the macrochelate across 50 residues. Only by raising the actual concentration of αSyn can coordination by His50 take place from a second αSyn molecule coordinating to the N-

terminal Cu^{2+} complex forming a ternary complex, rather than the formation of a macrochelate, Figure 7c. Our data indicates that at 100 μM and below the proportion of His50 chelation at the N-terminal Cu^{2+} complex will be minimal. Although the 3N1O complex (ternary or macro-chelate) could also be present in small amounts, at physiological concentrations the 2N2O complex dominates (Fig 1a).

Others have described His50 involvement at pH 6.5 [16c], we suggest that in this case interpretation of the data is incorrect. The study points to a 2N2O Cu^{2+} complex as seen in the MDV complex, but suggests that the nitrogen ligand is from His50 rather than the N-terminal amino group [16c]. This type of complex is extremely unlikely; there is a large body of evidence for αSyn, along with many other Cu^{2+} protein complexes that point to the N-terminal amino group anchoring Cu^{2+} complexes [24]. In particular, acetylation of the N-terminal amino group completely removes the strong coordination mode from αSyn [20].

The concentration dependent behavior we have identified suggests that at physiological concentrations of αSyn, His50 will not bind at the N-terminal complex, however self-association of αSyn might favor the ternary Cu^{2+} complex formation. This in turn will influence the αSyn fibril assembly pathway [8] and morphology[9a, 9b]. Recent high resolution cryo-EM structures of αSyn indicate that the His50 is distant from the N-terminus in the final fibril structures reported [25] even when you consider bridging ternary Cu^{2+} complexes between two αSyn molecules in the fibril structure.

The affinity of Cu^{2+} for αSyn is an important determinant of the physiological relevance of the interaction. Cu^{+} is tightly chaperoned and regulated within the cytosol while Cu^{2+} is more weakly bound extra-cellularly and it is believed Cu^{2+} reaches levels of 15 micromolar [26], some have reported even higher fluxes of Cu^{2+} at the synapse, from 20-250 micromolar, during neuronal

depolarization [27]. The 0.1 nM affinity (K_d) determined here for αSyn is therefore sufficiently tight to bind extracellular levels of Cu^{2+}.

The affinity measured here of 0.1 nM conditional dissociation constant for full-length αSyn at pH 7.4 (and for MDV 0.28 nM) is in agreement with a number of studies on full-length αSyn using a range of techniques: 0.2 nM at pH 7.4 [28]; 0.1 nM at pH 7.4 [16b]; and 0.4 nM at pH 7.0 [5b]. Others have reported affinities weaker than the 0.1 nM [15a, 29] but none have suggested an affinity (K_d) as tight as 0.03 nM observed for the model peptide αSyn(1-7,46-52) which can form the macro-chelate with Histidine. This further supports our assertion that Histidine50 does not stabilize the primary Cu^{2+} binding site in monomeric αSyn.

The affinity for our acetylated peptide containing a single histidine, αSyn(ac46-52) has been determined to have a K_d of 18 μM at pH 7.4, which is in agreement with other reports [30]. This peptide represents a model for Cu^{2+} binding to full-length acetylated–αSyn. The N-terminally acetylated peptide has a Cu^{2+} affinity five orders of magnitude weaker than non-acetylated αSyn.

Conclusion

We have shown that free imidazole or His50 within αSyn will only displace water as a ligand to the N-terminal Cu^{2+} complex at high (>350 μM) concentrations. This concentration dependent behavior gives an explanation for the seemingly conflicting observations made regarding the role of His50. Our studies show that, although αSyn is intrinsically disordered, forming a large macrochelate is not favored. Cu^{2+} coordination to the N-terminus together with His50 only takes place at higher, non-physiological, concentrations (used in EPR measurements) which results in a ternary complex, Figure 7c.

Cu^{2+} coordination to αSyn and its N-terminal acetylated form has been shown to accelerate fibril assembly [8, 10]. Cu^{2+} binding to the N-terminus can also impact the assembly pathway [8], fibril morphology [9a, 9b, 9c] and cytotoxicity [9b, 9c] of αSyn. How changes in metal homeostasis can impact the development of Parkinson's Disease is still an open question [2-3]. We still have much to discover surrounding the role of physiological metal ions in the amyloid assembly, redox chemistry and cytotoxicity of αSyn and other amyloidogenic proteins.

ASSOCIATED CONTENT

The following files are available free of charge. Supplementary Figures S1-S7 (PDF)

AUTHOR INFORMATION

Corresponding Author

John H Viles. School of Biological and Chemical Sciences, Queen Mary, University of London Mile End Road, London E1 4NS, UK

Author Contributions

‡These authors contributed equally.

Funding Sources

We are thankful for the support of the China Scholarship Council and the BBSRC; project grant code BB/M023877/1.

ACKNOWLEDGMENT

We are thankful for the support of the China Scholarship Council and the BBSRC; project grant code BB/M023877/1.

ABBREVIATIONS

αSyn, Alpha-synuclein; CD Circular Dichroism; PD, Parkinson’s disease

REFERENCES

1. (a) Polymeropoulos, M. H.; Lavedan, C.; Leroy, E.; Ide, S. E.; Dehejia, A.; Dutra, A.; Pike, B.; Root, H.; Rubenstein, J.; Boyer, R.; Stenroos, E. S.; Chandrasekharappa, S.; Athanassiadou, A.; Papapetropoulos, T.; Johnson, W. G.; Lazzarini, A. M.; Duvoisin, R. C.; DiIorio, G.; Golbe, L. I.; Nussbaum, R. L., Mutation in the alpha-synuclein gene identified in families with Parkinson's disease. *Science* **1997,** *276* (5321), 2045-2047; (b) Kruger, R.; Kuhn, W.; Muller, T.; Woitalla, D.; Graeber, M.; Kosel, S.; Przuntek, H.; Epplen, J. T.; Schols, L.; Riess, O., Ala30Pro mutation in the gene encoding alpha-synuclein in Parkinson's disease. *Nature Genetics* **1998,** *18* (2), 106-108; (c) Appel-Cresswell, S.; Vilarino-Guell, C.; Encarnacion, M.; Sherman, H.; Yu, I.; Shah, B.; Weir, D.; Thompson, C.; Szu-Tu, C.; Trinh, J.; Aasly, J. O.; Rajput, A.; Rajput, A. H.; Stoessl, A. J.; Farrer, M. J., Alpha-synuclein p.H50Q, a novel pathogenic mutation for Parkinson's disease. *Movement Disord* **2013,** *28* (6), 811-813.
2. Pall, H. S.; Blake, D. R.; Gutteridge, J. M.; Williams, A. C.; Lunec, J.; Hall, M.; Taylor, A., RAISED CEREBROSPINAL-FLUID COPPER CONCENTRATION IN PARKINSON'S DISEASE. *The Lancet* **1987,** *330* (8553), 238-241.
3. Gorell, J.; Johnson, C.; Rybicki, B.; Peterson, E.; Kortsha, G.; Brown, G.; Richardson, R., Occupational exposure to manganese, copper, lead, iron, mercury and zinc and the risk of Parkinson's disease. *Neurotoxicology* **1998,** *20* (2-3), 239-247.
4. (a) Binolfi, A.; Valiente-Gabioud, A. A.; Duran, R.; Zweckstetter, M.; Griesinger, C.; Fernandez, C. O., Exploring the Structural Details of Cu(I) Binding to alpha-Synuclein by NMR Spectroscopy. *Journal of the American Chemical Society* **2011,** *133* (2), 194-196; (b) Binolfi, A.; Quintanar, L.; Bertoncini, C. W.; Griesinger, C.; Fernández, C. O., Bioinorganic chemistry of copper coordination to alpha-synuclein: Relevance to Parkinson's disease. *Coordination Chemistry Reviews* **2012,** *256* (19–20), 2188-2201; (c) Valensin, D.; Dell'Acqua, S.; Kozlowski, H.; Casella, L., Coordination and redox properties of copper interaction with alpha-synuclein. *J Inorg Biochem* **2016,** *163*, 292-300.
5. (a) Wang, C.; Liu, L.; Zhang, L.; Peng, Y.; Zhou, F., Redox Reactions of the α-Synuclein−Cu2+ Complex and Their Effects on Neuronal Cell Viability. *Biochemistry* **2010,** *49* (37), 8134-8142; (b) Davies, P.; Wang, X.; Sarell, C. J.; Drewett, A.; Marken, F.; Viles, J. H.; Brown, D. R., The Synucleins Are a Family of Redox-Active Copper Binding Proteins. *Biochemistry* **2010,** *50* (1), 37-47; (c) Meloni, G.; Vašák, M., Redox activity of α-synuclein–Cu is silenced by Zn7-metallothionein-3. *Free Radical Biology and Medicine* **2011,** *50* (11), 1471-1479.
6. (a) Abeyawardhane, D. L.; Fernandez, R. D.; Heitger, D. R.; Crozier, M. K.; Wolver, J. C.; Lucas, H. R., Copper Induced Radical Dimerization of alpha-Synuclein Requires Histidine. *Journal of the American Chemical Society* **2018,** *140* (49), 17086-17094; (b) Al-Hilaly, Y. K.; Biasetti, L.; Blakeman, B. J. F.; Pollack, S. J.; Zibaee, S.; Abdul-Sada, A.; Thorpe, J. R.; Xue, W. F.; Serpell, L. C., The involvement of dityrosine crosslinking in alpha-synuclein assembly and deposition in Lewy Bodies in Parkinson's disease. *Sci Rep-Uk* **2016,** 6, 39171 ; (c) Gu, M.;

Bode, D. C.; Viles, J. H., Copper Redox Cycling Inhibits A beta Fibre Formation and Promotes Fibre Fragmentation, while Generating a Dityrosine A beta Dimer. *Sci Rep-Uk* **2018,** *8*, 16190.
7. (a) Borghi, R.; Marchese, R.; Negro, A.; Marinelli, L.; Forloni, G.; Zaccheo, D.; Abbruzzese, G.; Tabaton, M., Full length alpha-synuclein is present in cerebrospinal fluid from Parkinson's disease and normal subjects. *Neuroscience Letters* **2000,** *287* (1), 65-67; (b) Lee, S. J., Origins and effects of extracellular alpha-synuclein: Implications in Parkinson's disease. *J Mol Neurosci* **2008,** *34* (1), 17-22.
8. Zhang, H. Y.; Griggs, A.; Rochet, J. C.; Stanciu, L. A., In Vitro Study of alpha-Synuclein Protofibrils by Cryo-EM Suggests a Cu2+-Dependent Aggregation Pathway. *Biophys J* **2013,** *104* (12), 2706-2713.
9. (a) Uversky, V. N.; Li, J.; Fink, A. L., Metal-triggered Structural Transformations, Aggregation, and Fibrillation of Human α-Synuclein: A POSSIBLE MOLECULAR LINK BETWEEN PARKINSON′S DISEASE AND HEAVY METAL EXPOSURE. *Journal of Biological Chemistry* **2001,** *276* (47), 44284-44296; (b) Wright, J. A.; Wang, X.; Brown, D. R., Unique copper-induced oligomers mediate alpha-synuclein toxicity. *The FASEB Journal* **2009,** *23* (8), 2384-2393; (c) Choi, T. S.; Lee, J.; Han, J. Y.; Jung, B. C.; Wongkongkathep, P.; Loo, J. A.; Lee, M. J.; Kim, H. I., Supramolecular Modulation of Structural Polymorphism in Pathogenic -Synuclein Fibrils Using Copper(II) Coordination. *Angew Chem Int Edit* **2018,** *57* (12), 3099-3103.
10. (a) Rasia, R. M.; Bertoncini, C. W.; Marsh, D.; Hoyer, W.; Cherny, D.; Zweckstetter, M.; Griesinger, C.; Jovin, T. M.; Fernández, C. O., Structural characterization of copper(II) binding to α-synuclein: Insights into the bioinorganic chemistry of Parkinson's disease. *Proc. Natl. Acad. Sci. U. S. A.* **2005,** *102* (12), 4294-4299; (b) Binolfi, A.; Rasia, R. M.; Bertoncini, C. W.; Ceolin, M.; Zweckstetter, M.; Griesinger, C.; Jovin, T. M.; Fernandez, C. O., Interaction of alpha-synuclein with divalent metal ions reveals key differences: A link between structure, binding specificity and fibrillation enhancement. *Journal of the American Chemical Society* **2006,** *128* (30), 9893-9901; (c) Abeyawardhane, D. L.; Heitger, D. R.; Fernandez, R. D.; Forney, A. K.; Lucas, H. R., C-Terminal Cu-II Coordination to alpha-Synuclein Enhances Aggregation. *Acs Chemical Neuroscience* **2019,** *10* (3), 1402-1410.
11. Viles, J. H., Metal ions and amyloid fiber formation in neurodegenerative diseases. Copper, zinc and iron in Alzheimer's, Parkinson's and prion diseases. *Coordin Chem Rev* **2012,** *256* (19-20), 2271-2284.
12. (a) Martin, R. B., Optical properties of transition metal ion complexes of amino acids and peptides. *Metal ions in biological systems* **1974,** *1*, 129-156; (b) Stanyon, H. F.; Cong, X. J.; Chen, Y.; Shahidullah, N.; Rossetti, G.; Dreyer, J.; Papamokos, G.; Carloni, P.; Viles, J. H., Developing predictive rules for coordination geometry from visible circular dichroism of copper(II) and nickel(II) ions in histidine and amide main-chain complexes. *Febs Journal* **2014,** *281* (17), 3945-3954; (c) Klewpatinond, M.; Viles, J. H., Empirical rules for rationalising visible circular dichroism of Cu(2+) and Ni(2+) histidine complexes: Applications to the prion protein. *Febs Letters* **2007,** *581* (7), 1430-1434.
13. (a) Klewpatinond, M.; Davies, P.; Bowen, S.; Brown, D. R.; Viles, J. H., Deconvoluting the Cu2+ Binding Modes of Full-length Prion Protein. *J. Biol. Chem.* **2008,** *283* (4), 1870-1881; (b) Viles, J. H.; Cohen, F. E.; Prusiner, S. B.; Goodin, D. B.; Wright, P. E.; Dyson, H. J., Copper binding to the prion protein: Structural implications of four identical cooperative binding sites. *Proc. Natl. Acad. Sci. U. S. A.* **1999,** *96* (5), 2042-2047; (c) Stanyon, H. F.; Patel, K.; Begum, N.;

Viles, J. H., Copper(II) Sequentially Loads onto the N-Terminal Amino Group of the Cellular Prion Protein before the Individual Octarepeats. *Biochemistry* **2014,** *53* (24), 3934-3939.
14. Sung, Y. H.; Rospigliosi, C.; Eliezer, D., NMR mapping of copper binding sites in alpha-synuclein. *Bba-Proteins Proteom* **2006,** *1764* (1), 5-12.
15. (a) Binolfi, A. s.; Rodriguez, E. E.; Valensin, D.; D'Amelio, N.; Ippoliti, E.; Obal, G.; Duran, R.; Magistrato, A.; Pritsch, O.; Zweckstetter, M.; Valensin, G.; Carloni, P.; Quintanar, L.; Griesinger, C.; Fernández, C. O., Bioinorganic Chemistry of Parkinson's Disease: Structural Determinants for the Copper-Mediated Amyloid Formation of Alpha-Synuclein. *Inorganic Chemistry* **2010,** *49* (22), 10668-10679; (b) Kowalik-Jankowska, T.; Rajewska, A.; Wiśniewska, K.; Grzonka, Z.; Jezierska, J., Coordination abilities of N-terminal fragments of α-synuclein towards copper(II) ions: A combined potentiometric and spectroscopic study. *Journal of Inorganic Biochemistry* **2005,** *99* (12), 2282-2291; (c) Binolfi, A. s.; Lamberto, G. R.; Duran, R.; Quintanar, L.; Bertoncini, C. W.; Souza, J. M.; Cerveñansky, C.; Zweckstetter, M.; Griesinger, C.; Fernández, C. O., Site-Specific Interactions of Cu(II) with α and β-Synuclein: Bridging the Molecular Gap between Metal Binding and Aggregation. *J. Am. Chem. Soc.* **2008,** *130* (35), 11801-11812.
16. (a) Drew, S. C.; Ling Leong, S.; Pham, C. L. L.; Tew, D. J.; Masters, C. L.; Miles, L. A.; Cappai, R.; Barnham, K. J., Cu2+ Binding Modes of Recombinant α-Synuclein − Insights from EPR Spectroscopy. *J. Am. Chem. Soc.* **2008,** *130* (24), 7766-7773; (b) Dudzik, C. G.; Walter, E. D.; Millhauser, G. L., Coordination Features and Affinity of the Cu2+ Site in the α-Synuclein Protein of Parkinson's Disease. *Biochemistry* **2011,** *50* (11), 1771-1777; (c) Bortolus, M.; Bisaglia, M.; Zoleo, A.; Fittipaldi, M.; Benfatto, M.; Bubacco, L.; Maniero, A. L., Structural Characterization of a High Affinity Mononuclear Site in the Copper(II)-α-Synuclein Complex. *J. Am. Chem. Soc.* **2010,** *132* (51), 18057-18066; (d) Kowalik-Jankowska, T.; Rajewska, A.; Jankowska, E.; Grzonka, Z., Copper(II) binding by fragments of alpha-synuclein containing M-1-D-2- and -H-50-residues; a combined potentiometric and spectroscopic study. *Dalton T* **2006,** (42), 5068-5076.
17. De Ricco, R.; Valensin, D.; Dell'Acqua, S.; Casella, L.; Dorlet, P.; Faller, P.; Hureau, C., Remote His50 Acts as a Coordination Switch in the High-Affinity N-Terminal Centered Copper(II) Site of alpha-Synuclein. *Inorganic Chemistry* **2015,** *54* (10), 4744-4751.
18. Ohrfelt, A.; Zetterberg, H.; Andersson, K.; Persson, R.; Secic, D.; Brinkmalm, G.; Wallin, A.; Mulugeta, E.; Francis, P. T.; Vanmechelen, E.; Aarsland, D.; Ballard, C.; Blennow, K.; Westman-Brinkmalm, A., Identification of Novel alpha-Synuclein Isoforms in Human Brain Tissue by using an Online NanoLC-ESI-FTICR-MS Method. *Neurochemical Research* **2011,** *36* (11), 2029-2042.
19. Bartels, T.; Choi, J. G.; Selkoe, D. J., alpha-Synuclein occurs physiologically as a helically folded tetramer that resists aggregation. *Nature* **2011,** *477* (7362), 107-U123.
20. (a) Moriarty, G. M.; Minetti, C. A. S. A.; Remeta, D. P.; Baum, J., A Revised Picture of the Cu(II)-alpha-Synuclein Complex: The Role of N-Terminal Acetylation. *Biochemistry* **2014,** *53* (17), 2815-2817; (b) Miotto, M. C.; Valiente-Gabioud, A. A.; Rossetti, G.; Zweckstetter, M.; Carloni, P.; Selenko, P.; Griesinger, C.; Binolfi, A.; Fernandez, C. O., Copper Binding to the N-Terminally Acetylated, Naturally Occurring Form of Alpha-Synuclein Induces Local Helical Folding. *Journal of the American Chemical Society* **2015,** *137* (20), 6444-6447.
21. Fusco, G.; De Simone, A.; Gopinath, T.; Vostrikov, V.; Vendruscolo, M.; Dobson, C. M.; Veglia, G., Direct observation of the three regions in alpha-synuclein that determine its membrane-bound behaviour. *Nature Communications* **2014,** 5:3827.

22. Dawson, R.; Elliott, D.; Elliott, W.; Jones, K., *Data for Biochemical Research*. 3rd ed.; Clarendon Press: Oxford, UK, 1986.
23. Bryce, G. F.; Gurd, F. R. N., Visible Spectra and Optical Rotatory Properties of Cupric Ion Complexes of l-Histidine-containing Peptides. *Journal of Biological Chemistry* **1966,** *241* (1), 122-129.
24. (a) Patel, S. U.; Sadler, P. J.; Tucker, A.; Viles, J. H., Direct-Detection of Albumin in Human Blood-Plasma by 1h Nmr-Spectroscopy - Complexation of Nickel2+. *Journal of the American Chemical Society* **1993,** *115* (20), 9285-9286; (b) Barritt, J. D.; Viles, J. H., Truncated Amyloid-beta((11-40/42)) from Alzheimer Disease Binds Cu2+ with a Femtomolar Affinity and Influences Fiber Assembly. *Journal of Biological Chemistry* **2015,** *290* (46), 27791-27802.
25. (a) Li, B. S.; Ge, P.; Murray, K. A.; Sheth, P.; Zhang, M.; Nair, G.; Sawaya, M. R.; Shin, W. S.; Boyer, D. R.; Ye, S. L.; Eisenberg, D. S.; Zhou, Z. H.; Jiang, L., Cryo-EM of full-length alpha-synuclein reveals fibril polymorphs with a common structural kernel. *Nature Communications* **2018,** *9*, 3609; (b) Guerrero-Ferreira, R.; Taylor, N. M. I.; Mona, D.; Ringler, P.; Lauer, M. E.; Riek, R.; Britschgi, M.; Stahlberg, H., Cryo-EM structure of alpha-synuclein fibrils. *Elife* **2018,** *7*, 36402
26. Hartter, D. E.; Barnea, A., Evidence for release of copper in the brain: depolarization-induced release of newly taken-up 67copper. *Synapse* **1988,** *2* (4), 412-5.
27. (a) Kardos, J.; Kovacs, I.; Hajos, F.; Kalman, M.; Simonyi, M., Nerve endings from rat brain tissue release copper upon depolarization. A possible role in regulating neuronal excitability. *Neurosci Lett* **1989,** *103* (2), 139-44; (b) Brown, D. R.; Qin, K.; Herms, J. W.; Madlung, A.; Manson, J.; Strome, R.; Fraser, P. E.; Kruck, T.; von Bohlen, A.; Schulz-Schaeffer, W.; Giese, A.; Westaway, D.; Kretzschmar, H., The cellular prion protein binds copper in vivo. *Nature* **1997,** *390* (6661), 684-7.
28. Hong, L.; Simon, J. D., Binding of Cu(II) to Human α-Synucleins: Comparison of Wild Type and the Point Mutations Associated with the Familial Parkinson's Disease. *The Journal of Physical Chemistry B* **2009,** *113* (28), 9551-9561.
29. Jackson, M. S.; Lee, J. C., Identification of the Minimal Copper(II)-Binding α-Synuclein Sequence. *Inorganic Chemistry* **2009,** *48* (19), 9303-9307.
30. Valensin, D.; Camponeschi, F.; Luczkowski, M.; Baratto, M. C.; Remelli, M.; Valensin, G.; Kozlowski, H., The role of His-50 of alpha-synuclein in binding Cu(II): pH dependence, speciation, thermodynamics and structure. *Metallomics* **2011,** *3* (3), 292-302.

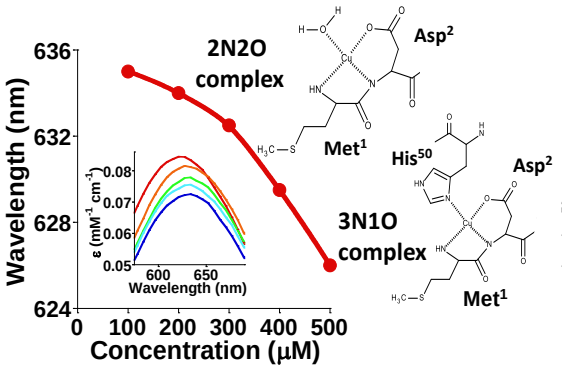

TOC:

Copper^{2+} Binding to α-Synuclein. Histidine50 can form a ternary complex with Cu^{2+} at the N-terminus but not a macrochelate.

Copper may impact α-Synuclein neurotoxicity in Parkinsons Disease. We have compared affinity, visible absorbance, visible circular-dichroism and pH dependence behavior for full-length α-Synuclein to that of a series of model peptides. We resolve a long standing controversy surrounding the role of His50 in Cu^{2+} coordination to α-Synuclein. We show that a ternary complex which involves the Cu^{2+} at the N-terminal and His50 only forms at higher concentrations, while a macrochelate is not favoured.